Joint International Topical Meeting on Mathematics & Computation and Supercomputing in Nuclear Applications (M&C + SNA 2007)
Monterey, California, April 15-19, 2007, on CD-ROM, American Nuclear Society, LaGrange Park, IL (2007)

BENCHMARKING WIMS/RFSP AGAINST MEASUREMENT DATA OF WOLSONG NUCLEAR POWER PLANTS

Chang Je Park and Hangbok Choi
Korea Atomic Energy Research Institute
Yuseong-gu, Deokjin-dong 150, Daejeon, Korea
cjpark@kaeri.re.kr; choih@kaeri.re.kr

ABSTRACT

Benchmark calculations of Canada deuterium uranium (CANDU) reactor physics design and analysis codes have been performed using the Phase-B measurement data of Wolsong nuclear power plants (NPP) 2, 3 and 4. At first, the lattices and reactivity device models were examined based on Wolsong NPP 2 measurement data for the criticality and reactivity device worth. Sensitivity calculations were also performed for the number of energy groups and the neutron weighting spectrum. Based on the results of the Wolsong NPP 2 calculation, the benchmark calculations were performed for Wolsong NPP 3 and 4. The results of this study showed that the criticality calculation matched the measurement result within 0.1%δk. The prediction errors of the reactivity device worth and thermal flux distributions were all within the allowed uncertainty.

Key Words: CANDU, Benchmark, WIMS-AECL, DRAGON, RFSP

1. INTRODUCTION

The design and analysis of a natural uranium Canada deuterium uranium (CANDU) reactor core are typically performed by a lattice code POWDERPUFS-V (PPV) [1] in conjunction with a supercell code MULTICELL [2] and a core analysis code RFSP [3]. The PPV code has been developed based on a series of physics measurements, but the application of PPV is limited to a natural uranium fuel because of the implemented empirical correlations. For an advanced CANDU fuel design and analysis [4-6], a transport code WIMS-AECL [7] is widely used owing to its modeling capability of a two-dimensional geometry and a diverse isotopic composition. In addition, instead of the MULTICELL code, a three-dimensional transport code DRAGON [8] is used for the generation of the incremental cross-sections of the reactivity devices.

In order to assess the performance of the physics analysis method based on the WIMS-AECL and RFSP code system, it is necessary to perform a benchmark calculation against experimental data. For a commercial CANDU nuclear power plant (NPP), the physics measurements are performed during the Phase-B commissioning period, which includes the first approach to a criticality and the low power tests necessary to verify the physics design and to evaluate the performance of the control and protective systems. In Korea, there are four 713 MWe CANDU (CANDU-6) NPP and the Phase-B test results of these plants are available from the Korea Hydro Nuclear Company [9-11]. In this study, the results of the Wolsong-2, 3 and 4 Phase-B tests are used for benchmarking the WIMS-AECL and RFSP codes. The results of the Wolsong-1 Phase-B tests are not used in this study because the uncertainty level was relatively large when the first physics measurements were performed.

In the previous studies, benchmark calculations were performed for Wolsong-2 NPP [12, 13]. Though the calculation results were, in general, consistent with the measurement, the off-criticality was relatively large when compared with the results by the PPV and RFSP codes. In this study, the lattice model of the standard CANDU fuel and the reactivity device model of the CANDU reactor were thoroughly investigated to establish reference lattice and reactivity device models based on the Wolsong-2 measurement results. Sensitivity calculations were performed for the material composition and then the criticality and the reactivity device worth were estimated. Using the reference lattice and reactivity device models, the benchmark calculations were performed for the Wolsong-2, 3 and 4 plants. The benchmark calculations included the predictions for the criticality, boron worth, reactivity device worth, reactivity coefficients, and the flux distribution.

2. CALCULATION MODEL

2.1. Lattice Model

The lattice parameters are generated by WIMS-AECL, which is a multi-group transport code for the fuel lattice and depletion calculations. For the CANDU fuel lattice calculation, the collision probability method was chosen to model the two-dimensional geometry exactly with an 89-group ENDF/B-V cross-section library. For the leakage calculation, the B1 method with the Benosit diffusion coefficient has been used. The multi-group cell-average cross-sections are collapsed into two-group lattice parameters by the WIMTAB program.

A standard CANDU fuel lattice has 37 natural uranium fuel rods as shown in Fig. 1. The fuel bundle is loaded in a fuel channel (or a pressure tube) and a calandria tube surrounds the pressure tube which physically separates the moderator from the coolant. The specifications of the fuel bundle and lattice are given in Table I. For the lattice calculation, the material compositions of the clad (Zr-2), pressure tube (Zr-2.5%Nb) and calandria tube (Zr-2) were obtained from a website [14-16]. For the clad and calandria tube material, however, the tin (Sn) was replaced by phosphorus (^{31}P) because the WIMS-AECL library doesn't have cross-sections for tin.

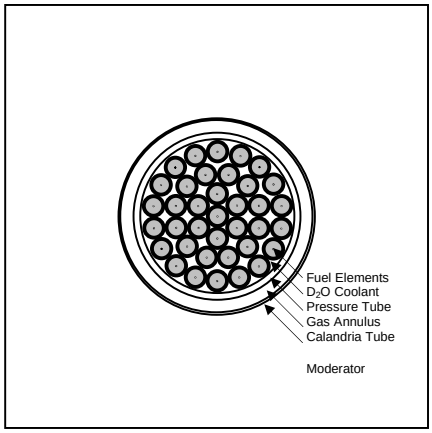

Figure 1. A CANDU fuel bundle lattice model.

Table I. Specifications of the CANDU fuel lattice.

Fuel bundle		Fuel lattice	
Fuel material	UO_2	Lattice pitch (cm), square	28.575
Number of fuel rods	37	Pressure tube (Zr-2.5% Nb) inside diameter (cm)	10.3378
Rod outside diameter (cm)	1.31	Pressure tube wall thickness (cm)	0.4343
Average clad wall thickness (cm)	0.04	Calandria tube (Zr-2) inside diameter (cm)	12.8956
Pellet outside diameter (cm)	1.22	Calandria tube wall thickness (cm)	0.1397
Pellet density (g/cm^3)	10.6		
^{235}U content (wt%)	0.711		
Stack length (cm)	48.2		

2.2. Reactivity Device Model

There are four major reactivity devices in the CANDU-6 reactor such as an adjuster (ADJ), shutoff rod (SOR), mechanical control absorber (MCA), and a light water zone controller unit (ZCU), which are shown in Fig. 2. There are also many other structural materials that support these devices in the reactor core as summarized in Table II. These reactivity devices and structural materials are represented by incremental cross-sections in the reactor analysis by the RFSP code. The incremental cross-section is a difference of the homogenized cross-sections of a 3-dimensional fuel lattice with and without a reactivity device, which is obtained by the DRAGON code. The conceptual model of the reactivity device by the DRAGON code is shown in Fig. 3.

Table II. Number of reactivity devices.

Adjusters	21	Liquid poison injection nozzles	6
Light water zone control units	6	Vertical flux detector assemblies	26
Mechanical control absorbers (Cd)	4	Horizontal flux detector assemblies	7
Shutoff rods (Cd)	28		

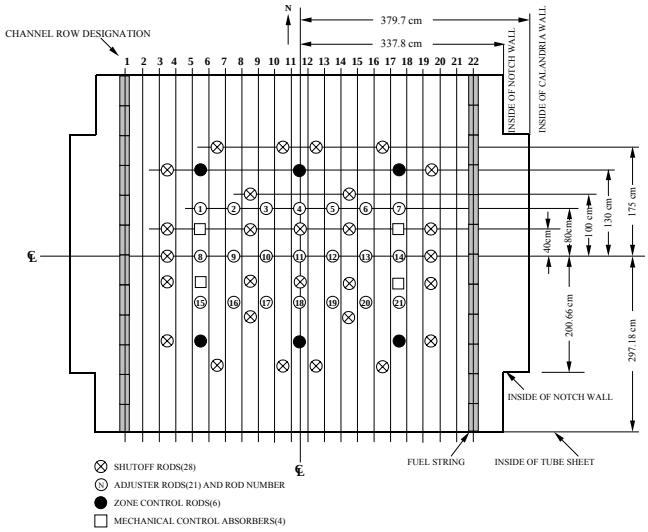

Figure 2. Location of the reactivity devices (top view).

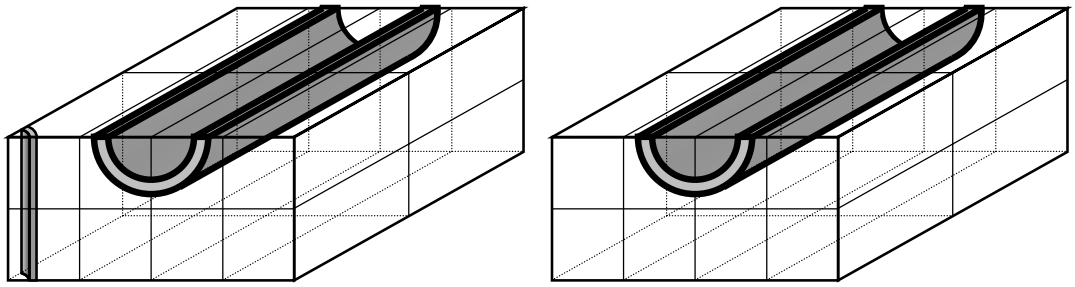

(a) Reactivity device (b) Fuel channel

Figure 3. Reactivity device model by DRAGON.

2.3. Core Calculation Model

The core calculation is performed by the RFSP which is a three-dimensional diffusion code. In the RFSP code, the finite-difference model is used to divide the reactor core, including the reflector region, into rectangular parallelepipeds (nodes). The basic mesh structure is a one lattice pitch (LP) by one LP in the XY plane and one bundle length (BL) in the axial direction, respectively. In the X-direction, one LP is typically divided into two numerical meshes in the core central region. In the Y- and Z-directions, the meshes have been set to describe the reactivity devices and the fuel bundle correctly. For a fresh core, two depleted uranium fuel bundles are loaded into a fuel channel at bundle positions 8 and 9 in the 80 central fuel channels, which flattens both the radial and axial power distributions. Because the CANDU reactor adopts a bi-directional fueling scheme, the distribution of the depleted uranium fuel bundles is symmetric about the axial mid-plane of the core. The general specification of the CANDU-6 reactor core is described in Table III.

Table III. Design data of a nominal CANDU-6 reactor core.

Number of fuel channels	380	Length of calandria notch (cm)	96.52
Length of a fuel channel (cm)	594.4	Reactor core radius (cm)	314.3
Inner radius of main calandria (cm)	379.7	Reflector thickness (cm)	65.6
Inner radius of subcalandra (cm)	337.8		

3. SENSITIVITY CALCULATION OF THE ANALYSIS MODEL

3.1. Sensitivity of the Material Data

The lattice model was examined for its geometry and material composition. The present model assumes that the clad and fuel gap are mixed by reducing the clad material number density. A comparison of a homogeneous and an explicit model for the fuel gap showed that a homogenization of a fuel gap with a clad had a negligible effect on the eigenvalue. Then the effect of material data was examined as summarized in Table IV by updating the material

compositions one by one. For the clad and calandria tube material, the natural zirconium content was changed from 99.71 wt% to 98.5 wt%. For the pressure tube, the parasite absorber (natural boron) was replaced by 0.14 wt% of ^{16}O. For the Zircaloy-2, the old model used natural boron to represent the tin. In the present model, the tin was replaced by ^{31}P and the content was adjusted based on the thermal absorption cross-section. The helium density was reduced from 0.0014 g/cm^3 to 0.0001785 g/cm^3. The natural boron content (9 ppm) in the moderator was evaluated more accurately. Finally the composition of the end plate, which is assumed to be a mixture of the clad and moderator material in the present model, was adjusted by considering all the modifications. The effect of the material composition was estimated for the infinite and effective multiplication factors of the fuel lattice as well as the effective multiplication factor of the core.

Table IV. Sensitivity of the material composition data.

	WIMS-AECL				RFSP
	k_∞	Δk (mk)	k_{eff}	Δk (mk)	
Previous model [12, 13]	1.05241	-	1.03004	-	0.99823
(1) Clad Zr-2 update	1.05304	0.63	1.03065	0.61	0.99881
(2) Calandria tube Zr-2 update	1.05401	0.97	1.03160	0.95	0.99971
(3) Pressure tube Zr-Nb update	1.05629	2.28	1.03379	2.19	1.00182
(4) ^{31}P for Sn	1.05583	-0.46	1.03335	-0.44	1.00140
(5) Helium density	1.05582	-0.01	1.03312	-0.23	1.00114
(6) Moderator boron	1.05506	-0.76	1.03241	-0.71	1.00046
(7) End plate	1.05429	-0.77	1.03158	-0.83	0.99962

The sensitivity calculation of the material data showed that the zircaloy data used in the previous study had a non-negligible effect on the calculation result of the multiplication factors. Especially a dummy material that represents the impurities should be selected very carefully by considering the thermal absorption cross-section profile and the content should be adjusted accordingly. When these data are revised, the critical boron concentration can be predicted with an error of less than 0.1%.

3.2. Sensitivity of the Calculation Model

There are also fundamental parameters that should be determined to obtain more robust simulation results such as the number of energy groups, cross-section library and the weighting spectrum of the incremental cross-section generation. Therefore sensitivity calculations were performed on these parameters and the results were compared with the measurement data of the Wolsong-2 Phase-B test in Table V. The Phase-B core conditions of the Wolsong-2 NPP are as follows:

- The critical boron concentration is 9.0±0.5 ppm.
- The average temperature of the coolant and moderator are 308.12 and 302.16 °K, respectively.
- The average ZCU water level is 16.94%.
- The purity of the coolant and moderator are 99.63 and 99.84 wt%, respectively.
- The MCA is inserted by 55%.

Table V. Comparison of the reactivity device worth.

	Measured	Case A	Case B	Case C	Case D
ZCU (20%-60%)	0.07166 mk/%	0.07494 (4.6%)	0.07799 (8.8%)	0.07251 (1.2%)	0.07166 (0.0%)
ZCU (20%-80%)	0.06769 mk/%	0.07089 (4.7%)	0.07352 (8.6%)	0.06841 (1.1%)	0.06614 (-2.3%)
ADJ	10.879 mk	11.013 (1.2%)	10.903 (0.2%)	10.344 (-4.9%)	10.594 (-2.6%)
MCA	7.713 mk	8.865 (14.9%)	8.786 (13.9%)	8.224 (6.6%)	8.178 (6.0%)
SOR	45.378 mk	51.533 (13.6%)	51.062 (12.5%)	47.734 (5.2%)	47.446 (4.6%)

Case a) 1.5 energy groups, ENDF/B-V library, and natural uranium spectrum
Case b) 1.5 energy groups, ENDF/B-VI library, and natural uranium spectrum
Case c) 2 energy groups, ENDF/B-VI library, and natural uranium spectrum
Case d) 2 energy groups, ENDF/B-VI library, and natural/depleted uranium spectrum.

For the CANDU reactor physics analysis, a 1.5-group model is typically used, in which the fast fission and up-scattering cross-sections are added to the thermal fission and down-scattering cross-sections, respectively, by a flux-volume weighting. Though the 1.5-group is generally acceptable for a well-thermalized system like a CANDU reactor, a 2-group model is now being used not only for the existing CANDU reactors but also for an advanced CANDU reactor design and analysis.

For the reactivity device worth, it was found that the prediction results improved as the number of energy groups was increased from 1.5 to 2. Especially for the strong absorbers such as the MCA and SOR, it is mandatory to use the 2-group model to obtain credible results. For a grey absorber such as ADJ, the effect of the number of energy groups was relatively small. The effect of using a depleted uranium neutron spectrum when generating the incremental cross-section was not significant for the reactivity devices located near the depleted uranium fuel. The effect of using an ENDF/B-VI library was also small when compared to that of the number of energy groups. For the prediction of the thermal flux distribution, the trend was also similar to that of the reactivity device worth calculation.

4. BENCHMARK CALCULATION OF WOLSONG-2, 3 AND 4

The benchmark calculation was performed against the Phase-B physics measurement data of the Wolsong-2, 3 and 4 NPP. The initial core conditions of these plants are summarized in Table VI and the benchmark calculations were performed for the following cases:

- Approach to the first criticality,
- Calibration of the ZCU reactivity worth,
- Estimation of the reactivity device worth (ADJ, MCA, and SOR), and
- Thermal flux distribution.

Table VI. Phase-B core conditions.

	Wolsong-2	Wolsong-3	Wolsong-4
Critical boron concentration (ppm)	9	8.93	9.342
Averaged zone controller level (%)	16.94	15.44	15.75
MCA inserted (%)	55	55	45
Coolant temperature (°C)	34.96	32.15	34.3625
Moderator temperature (°C)	29.50	37.74	34.03
Coolant Purity (wt%)	99.63	99.24	99.27
Moderator Purity (wt%)	99.84	99.81	99.83

4.1. Critical Boron Concentration

The effective multiplication factors were estimated to be 0.99962, 0.99969 and 0.99812 for Wolsong-2, 3 and 4, respectively, and the corresponding critical boron concentrations were 8.98, 8.91 and 9.29. Therefore the critical boron concentrations are predicted with an excellent accuracy, which is within the uncertainty of the measured boron concentration (0.5 ppm).

4.2. Reactivity Device Worth

Because the ZCU worth was calibrated by using the boron concentration change in the moderator, the boron reactivity coefficient was calculated first. The boron reactivity coefficients were 7.67, 7.66 and 7.70 mk/ppm for Wolsong-2, 3 and 4, respectively. During the Phase-B test, the calibration of the ZCU was performed by dissolving a boron batch in the moderator. After one batch was added, the average ZCU water level was fitted in order to maintain the criticality. The estimated average ZCU level worth is given in Table VII and compared with the measurement results for typical operating ranges. The maximum error of the ZCU level worth is ~8%, which is smaller than the allowed uncertainty of ±10%.

Table VII. Calibration of the zone controller unit.

ZCU level (%)	Wolsong-2		Wolsong-3		Wolsong-4	
	Measured	Calculated	Measured	Calculated	Measured	Calculated
20~60	0.07166	0.07368 (2.8%)	0.07423	0.07630 (2.8%)	0.06807	0.07333 (7.7%)
20~80	0.06769	0.06938 (2.5%)	0.07050	0.07230 (2.5%)	0.06523	0.07028 (7.7%)

The reactivity worth of the individual ADJ rod was calculated and the largest error of the reactivity worth between the calculation and measurement was ~15%, while the error of the total ADJ worth was ~2%. The maximum error of the individual MCA was ~18%, while the error of the total MCA worth was ~8%. The maximum error of the individual SOR worth was ~15%, while the error of the total SOR worth was ~9%. For the reactivity device, the prediction error of

the total reactivity worth was within the allowed uncertainty of ±15%. For the strong absorbers such as the MCA and SOR, it was found that the reactivity worth was over-estimated by the WIMS/RFSP, which could be due to a poor estimation of the thermal flux depression in the absorber region.

4.3. Reactivity Coefficients

For the heat transport system (HTS) temperature coefficient measurement, the moderator temperature was fixed at 35ºC. The coolant and fuel temperatures were the same and they were varied from 35 to 260ºC. The corresponding coolant densities were calculated for D_2O at the saturated and non-boiling conditions with 99.63, 99.24 and 99.27 wt% purities for Wolsong-2, 3 and 4, respectively. The variation of the HTS temperature coefficient is shown in Fig. 4. The HTS temperature coefficient is generally consistent with the measured data.

For the moderator temperature coefficient (MTC), the coolant and fuel temperatures were fixed at 260ºC. The MTC was calculated by decreasing the temperature from 69 to 35ºC. The moderator density was calculated for D_2O at the saturated and non-boiling conditions with 99.84, 99.81 and 99.84 wt% purities for Wolsong-2, 3 and 4, respectively. The variation of the MTC is shown in Fig. 5. Compared with the measured data, the simulation error was relatively large (~20%). It is believed that this error is due to an inconsistent measurement procedure.

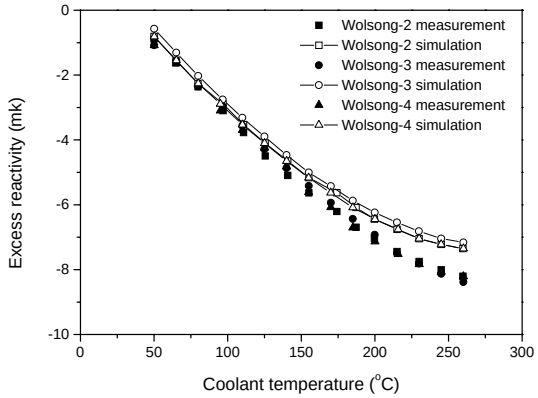

Figure 4. Coolant temperature coefficient.

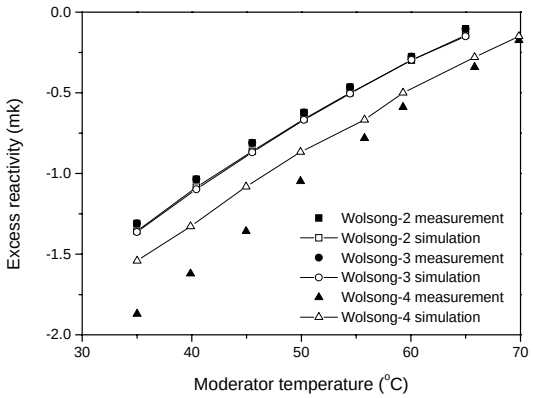

Figure 5. Moderator temperature coefficient.

4.4. Flux Distribution

During the Phase-B test, thermal flux scans were performed several times for various reactor configurations. This flux measurement confirms the physics design method and, in particular, the effects of various reactivity devices and the depleted uranium fuel on the neutron flux distributions. Flux scans along a chord of the reactor core were made with fission chamber mapping detectors. Vertical fission chamber scans were performed along 26 vertical flux detector (VFD) assemblies. Horizontal fission chamber scans were carried out along the horizontal flux detector (HFD) tube. The flux scan calculations were performed for the following cases:

(Case 1) Nominal case (with all ADJs),

(Case 2) MCA bank 1 inserted by 50% with ADJs,
(Case 3) MCA all inserted with ADJs,
(Case 4) Without ADJ bank 1, 2, 3 and 4,
(Case 5) Without all ADJs.

The ZCU water level was fixed at 40% and the moderator boron concentration was 8.5 ppm. The flux calculations were performed by using the INTREP module of the RFSP code. The flux scan calculations were performed for VFD 19 and HFD 1 for the vertical and horizontal fluxes, respectively. In order to obtain a flux at a detector position, a shape function was generated for a flux variation between the fuel channels and the horizontal and vertical thermal fluxes were corrected by using this shape function. The root-mean-square (RMS) errors of the flux calculation are summarized in Table VIII. The measured and calculated thermal fluxes are shown in Figs. 6 to 8 for the nominal case (Case 1).

Table VIII. Root-mean-square error of the flux scan

	Wolsong-2		Wolsong-3		Wolsong-4	
	Vertical	Horizontal	Vertical	Horizontal	Vertical	Horizontal
Case 1	5.9%	11.9%	10.4%	6.9%	7.9%	8.9%
Case 2	7.9%	9.2%	11.1%	6.6%	4.9%	8.2%
Case 3	9.4%	6.1%	6.3%	10.8%	5.0%	8.8%
Case 4	6.8%	6.7%	10.9%	9.7%	5.2%	8.1%
Case 5	7.1%	6.6%	8.2%	9.4%	6.5%	4.8%

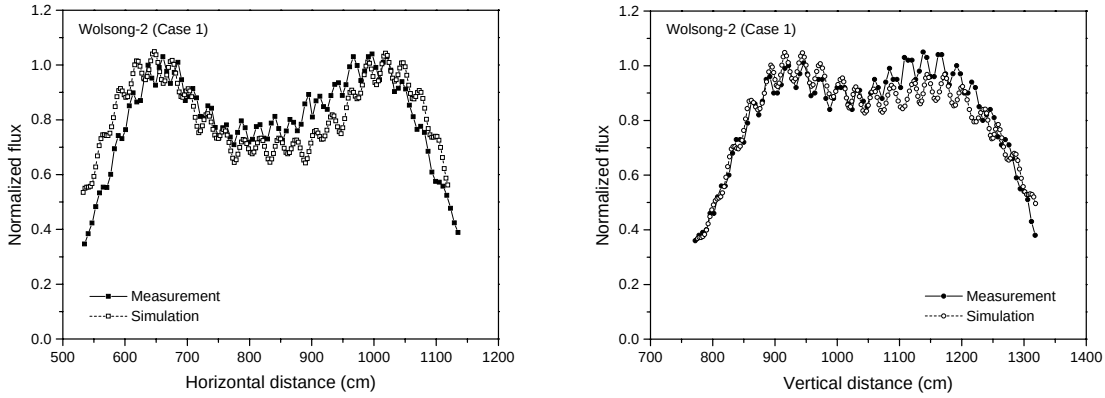

Figure 6. Comparison of the thermal fluxes for Wolsong-2 Case 1.

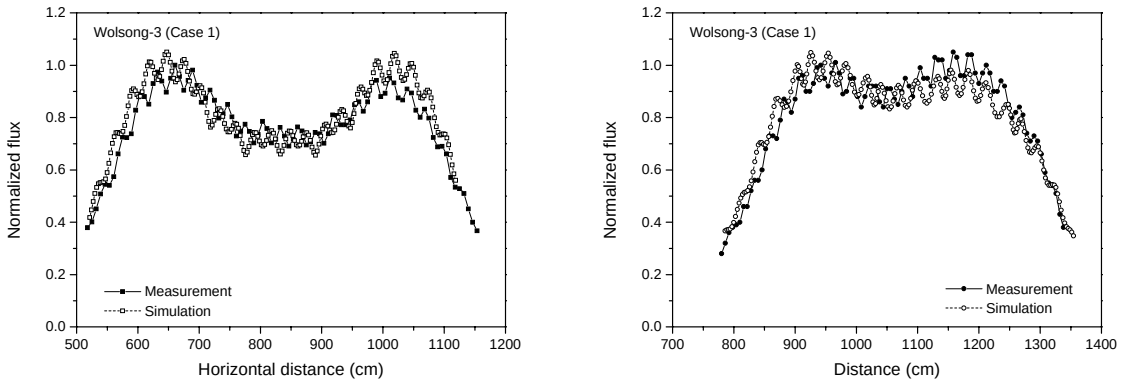

Figure 7. Comparison of the thermal fluxes for Wolsong-3 Case 1.

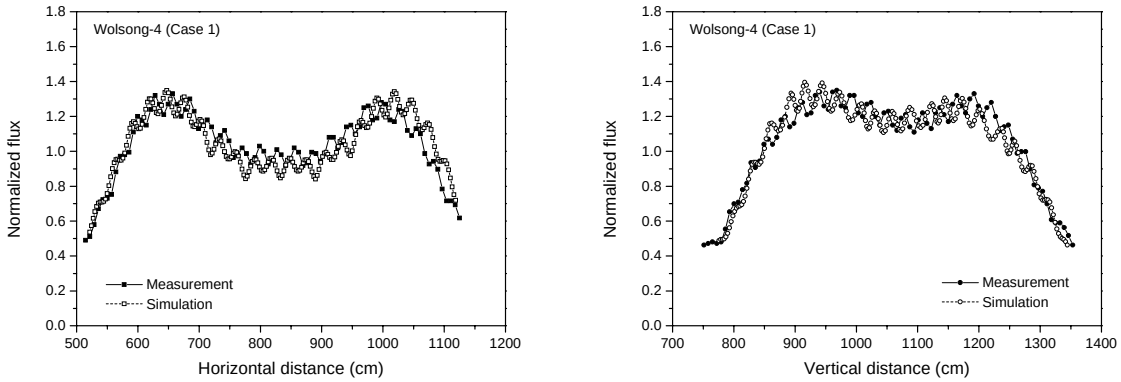

Figure 8. Comparison of the thermal fluxes for Wolsong-4 Case 1.

5. SUMMARY AND CONCLUSION

Benchmark calculations for typical CANDU physics design and analysis tools were performed based on the Phase-B measurement data of the Wolsong-2, 3 and 4 NPP. In this study, the benchmark calculations were done for the criticality, boron worth, reactivity device worth, reactivity coefficient, and the flux scan. For the lattice calculation, the 89-group ENDF/B-V library was used by the WIMS-AECL code. The benchmark calculation results showed that the criticality was predicted well by the WIIMS-AECL, DRAGON and RFSP. The total reactivity device worth was also predicted within the allowed uncertainty of the measured value. The heat transport system temperature coefficient showed an excellent agreement with the measured data and the flux distributions were also in good agreement with the measurement. However, the moderator temperature coefficient showed a relatively large error.

ACKNOWLEDGMENTS

This work has been carried out under the Nuclear Research and Development program of Korea Ministry of Science and Technology.

REFERENCES

1. E. S. Y. Tin and P. C. Loken, "POWDERPUFS-V Physics Manual," TDAI-31 Part 1, Atomic Energy of Canada Limited (1979).
2. A. R. Dastur, J. V. Marczak, F. Piva and J. V. Donnelly, "MULTICELL User's Manual," TDAI-208, Atomic Energy of Canada Limited (1979).
3. D. A. Jenkins and B. Rouben, "Reactor Fuelling Simulation Program - RFSP: User's Manual for Microcomputer Version," TTR-321, Atomic Energy of Canada Limited (1993).
4. P. G. Boczar, M. J. N. Gagnon, P. S. W. Chan, R. J. Ellis, R. A. Verrall and A. R. Dastur, "Advanced CANDU Systems for Plutonium Destruction," *Canadian Nuclear Society Bulletin*, **18** (1997).
5. P. G. Boczar, P. S. W. Chan, G. R. Dyck, R. J. Ellis, R. T. Jones, J. D. Sullivan and P. Taylor, "Thorium Fuel Cycle Studies for CANDU Reactors," IAEA-TECODC-1319, pp.25-41, International Atomic Energy Agency (2002).
6. M. S. Yang, H. Choi, C. J. Jeong, K. C. Song, J. W. Lee, G. I. Park, H. D. Kim, W. I. Ko, J. J. Park, K. H. Kim, H. H. Lee and J. H. Park, "The Status and Prospect of the DUPIC Fuel Technology," *Nuclear Engineering and Technology*, **38**, pp.359-374 (2006).
7. J. V. Donnelly, "WIMS-CRNL: A User's Manual for the Chalk River Version of WIMS", AECL-8955, Atomic Energy of Canada Limited (1986).
8. G. Marleau, A. Hébert and R. Roy, "A User Guide for DRAGON," IGE-174 Rev. 5, École Polytechnique de Montréal (2000).
9. S. M. Kim and H. W. Kim, "Wolsong NPP 2 Phase-B Test Post Simulation Report," Wolsong Nuclear Power Plant (1997).
10. S. C. Park, "Wolsong NPP 3 Phase-B Test Post Simulation Report," Wolsong Nuclear Power Plant (1998).
11. S. C. Park, "Wolsong NPP 4 Phase-B Test Post Simulation Report," Wolsong Nuclear Power Plant (1998).
12. H. Choi, G. Roh and D. Park, "Benchmarking MCNP and WIMS/RFSP Against Measurement Data – II: Wolsong Nuclear Power Plant 2," *Nucl. Sci. Eng.*, **150**, pp.37-55 (2005).
13. C. J. Park and H. Choi, "A Comparative Study on the CANDU-6 Reactivity Device Model Based on Wolsong-2 Physics Measurement Data," *Proceedings of PHYSOR 2006, ANS Topical Meeting on Reactor Physics*, Vancouver, Sept. 10-14 (2006).
14. "Material Property Data: Zircaloy-2 Zirconium Alloy, Zr-2.5Nb Zirconium Alloy, AISI Type 304L Stainless Steel, Special Metals INCONEL Alloy X-750," http://www.matweb.com/search (2006).
15. "Periodic Table of the Elements: Boron," http://chemistry.about.com/library (2006).
16. "Property of Common Gas Materials," http://www.efunda.com/materials/common_matl (2006).